IOP Publishing Superconductor Science and Technology
Supercond. Sci. Technol. 31 (2018) 015014 (10pp) https://doi.org/10.1088/1361-6668/aa9802

Evidence of pinning crossover and the role of twin boundaries in the peak effect in FeSeTe iron based superconductor

A Galluzzi[1,2], K Buchkov[3], V Tomov[3], E Nazarova[3], A Leo[1,2], G Grimaldi[2], A Nigro[1,2], S Pace[1,2] and M Polichetti[1,2]

[1] Department of Physics 'E.R. Caianiello', University of Salerno, via Giovanni Paolo II, 132, Fisciano (SALERNO), I-84084, Italy
[2] CNR-SPIN Salerno, via Giovanni Paolo II, 132, Fisciano (SALERNO), I-84084, Italy
[3] Institute of Solid State Physics, Bulgarian Academy of Sciences, 72 Tzarigradsko Chaussee Blvd., 1784 Sofia, Bulgaria

E-mail: polimax@sa.infn.it

Received 22 August 2017, revised 2 November 2017
Accepted for publication 3 November 2017
Published 5 December 2017

Abstract

The correlation between the appearance of a peak effect in the critical current of a superconducting material and the presence of twin boundaries, involved in a crossover between different pinning regimes, is investigated by means of dc magnetic measurements on a $FeSe_{0.5}Te_{0.5}$ crystal. In particular, by analyzing the temperature dependence of the critical current density $J_c(T)$ for different magnetic fields H, a crossover from a weak pinning regime to a strong pinning regime has been revealed. The analysis shows that this crossover can be ascribed to the presence of twin boundary defects inside the sample, and can be associated to the onset of the peak effect and interpreted as the start of the vortex dynamic processes responsible for the increase of J_c with the field. On the basis of the information extracted by our analysis, a plausible dynamic scenario involving the contribution of the different pinning regimes depending on the applied field has been described, and the relative H (T) vortex phase diagram has been determined. Moreover, in our description, the peak in the $J_c(H)$ curve corresponds to the end of the processes leading to the peak effect and it is confirmed to be related to the transition from an elastic to a plastic deformation regime in the vortex lattice.

Keywords: iron based superconductors, peak effect, dc magnetic properties, vortex dynamics, pinning crossover, twin boundaries, magnetism and superconductivity

(Some figures may appear in colour only in the online journal)

1. Introduction

The magnetic and electro-transport properties of all type-II conventional and non-conventional superconductors are determined by the complexity of the mixed state nature. Its aspects are very important from both fundamental and practical perspectives. The sophisticated features of the vortex matter and the diversity of phases, transitions and dynamical processes are shaped by numerous factors such as thermal fluctuations, anisotropy effects, inter-vortex interactions and the pinning topology formed by correlated and random structural disorder of the superconductor [1–3].

One of the most intriguing vortex phenomena is the second magnetization peak effect in the magnetic hysteresis (named the peak or 'fishtail' effect) originating from distinct non-linear modulations of the temperature and magnetic field dependencies of the critical current $J_c(H, T)$ due to pinning energy changes [4–6]. The proposed mechanisms and theoretical models deal particularly with the vortex–vortex and pinning center–vortex interactions as order/disorder phase transition (long/short range ordering) [7], structural (square/rhombic lattice) transformation [8], elastic/plastic pinning crossover [6] and 3D/2D pinning change [9]. The peak effect has been thoroughly investigated for various superconductor

systems: (i) conventional, like Nb alloys [10] and MgB_2 [11], and (ii) non-conventional such as cuprates [6, 12] and iron based superconductors (IBSs), both pnictides [13–17] and chalcogenide FeSeTe systems [18].

The study of the nature of the peak effect in IBSs is especially challenging due to the incomplete picture of the aforementioned vortex phenomena and the high potential of these materials for power application. In the iron-chalcogenide family, the FeSeTe system ($T_c = 14.5$ K) [19] (derivative of the basic FeSe [20]) has particular potential thanks to its chemical stability, superior critical parameters and pinning capabilities, leading to strong transport current performance at high magnetic fields [21–24].

The vortex matter in FeSeTe, and particularly the peak effect, have been investigated in detail mainly in single crystals [25–37]. It is important to note that the nature of the observed effects is strongly influenced by the material structure (Fe excess and Se/Te stoichiometric ratio) and sample morphology (amount and type of structural disorder), even for identically prepared crystals. Various mechanisms for the peak effect have been considered in FeSeTe: dominant weak δl type (due to spatial variation of the charge carrier mean free path) pinning with disorder-driven order/disorder transition from elastic to plastic pinning as reported in [27, 29, 30, 33], while other studies make claims for a δT_c (arising from local variations of T_c) type of pinning, resulting in a broad peak effect [38]. A mixture of δl and δT_c types of pinning and elastic to plastic transitions is reported by Tamegai *et al* [35]. Bonura *et al* [37] observe δl type single pinning crossover (low fields) to strongly interacting vortices (high fields). Other studies on FeSeTe with peak effect using Dew-Hughes analysis [39] identify the presence of normal core point pinning centers, probably related to Fe-inclusion clusters, inhomogeneous Te dopant distribution and/or planar strong pinning centers (twin boundaries) [31–33, 38], and finally even quantum creep effects [27]. It seems that in this case the peak effect is of a field-induced type as a consequence of the active role of the twin boundaries as strong pinning centers at high magnetic fields [40]. Reasonably, these are very sought-after from a practical point of view and in most cases are artificially engineered by means of irradiation, cluster inclusions (nanoparticles/secondary phases) and twin boundaries [1]. In materials such as YBCO [41] and BaFeCoAs [42], the specific orthorhombic structure favors the formation of twin boundaries, thus leading to the establishment of natural (correlated) structure disorder. A similar aptitude is also expected in the case of FeSeTe. The twin boundary regions reveal quite different behavior regarding the stability of the superconducting state in IBS systems: improved in pnictides [42] and suppressed in chalcogenides [43].

The current study is focused on the investigation of the peak effect and the magnetic phase diagram, which is shaped by the influence of different (weak and strong) pinning centers in the Bridgman grown FeSeTe twinned single crystal. For this purpose we have used an alternative approach for this compound based on the analysis of the temperature dependencies of the critical current density [1, 44–48] extended to the entire interval of field for identifying the regions of weak/strong pinning centers activity and the corresponding phases in the magnetic phase diagram.

2. Experimental details

We analyzed a $FeSe_{0.5}Te_{0.5}$ (nominal composition) twinned single crystal sample with dimensions $3 \times 3 \times 0.2\,mm^3$, fabricated by means of the Bridgman technique. A mixture of high purity Fe (99.9%), Se (99.998%) and Te (99.99%) powders with initial stoichiometry ratio 1:0.5:0.5 was weighed and homogenized (for 2 h) under an inert atmosphere in a glove box and then sealed in double quartz ampules evacuated at 10^{-5} Torr. The following growth procedure was used: 36 h at 1070 °C followed by a very slow rate of pulling, $2\,mm\,h^{-1}$, through the 1070 °C–700 °C temperature gradient of the Bridgman furnace, followed by 100 h of annealing at 400 °C and then furnace cooling to room temperature. The morphology and final chemical composition of the crystals was studied via SEM-EDX analysis. This revealed a slightly deviated final stoichiometric ratio $Fe_{0.96}Te_{0.59}Se_{0.45}$, probably a consequence of the appearance of micro-inhomogeneity and phase separation of magnetic premises, which is typical for crystal growth and synthesis in FeSeTe [49–52] and in the basic compound FeSe [53–55]. It is worth underlining that, according to the stoichiometry of 11 chalcogenides, the use of the notation 'Fe-Se-Te' could be more appropriate than 'FeSeTe'. However, here we prefer to use the nomenclature commonly used in the present literature to identify this family of materials.

The crystal was characterized by means of dc magnetic measurements, although fundamental and third harmonic ac susceptibility characterizations (not reported) were also performed to exclude the eventual presence of electromagnetic granularity in the detected magnetic response [56–59]. For the dc magnetic analysis the field was applied perpendicular to its largest face, and the dc magnetization as a function of the temperature $M(T)$ and of the dc magnetic field $M(H)$ were measured, using a Quantum Design PPMS-9T equipped with a VSM option. In order to avoid the residual trapped field inside the PPMS dc magnet affecting the sample response [60], this was reduced to below 3×10^{-4} T before each $M(T)$ following the procedure described in a previous paper [61].

The $M(T)$ measurements were performed in zero field cooling (ZFC)–field cooling (FC) conditions. More precisely, the sample was first cooled down to 2.5 K in the absence of the magnetic field, then the field was switched on and the data were acquired for increasing temperature (ZFC) up to 300 K. After that, the sample was cooled down again while acquiring FC magnetization.

For the $M(H)$ measurements, the sample was first cooled down to the measurement temperature in the absence of the field and thermally stabilized for at least 20 min. Then, the field was ramped with a sweep rate of $1 \times 10^{-2}\,T\,s^{-1}$ to

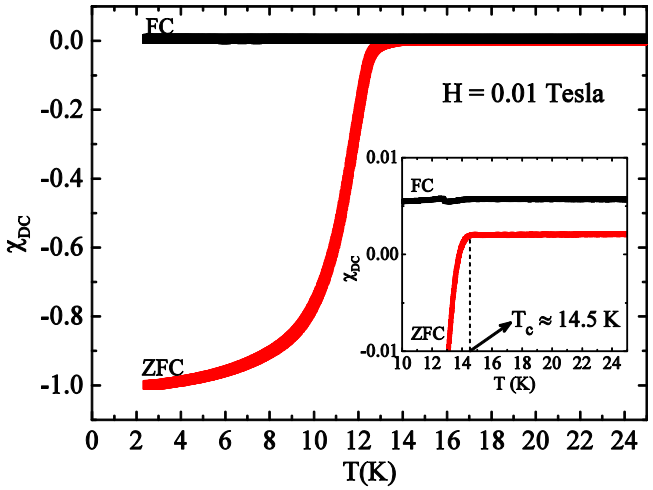

Figure 1. Dc susceptibility curve $\chi_{dc}(T)$ obtained from performing ZFC–FC procedure with an applied magnetic field of 0.01 T. Inset: an enlargement of the ZFC–FC curve near the superconducting transition.

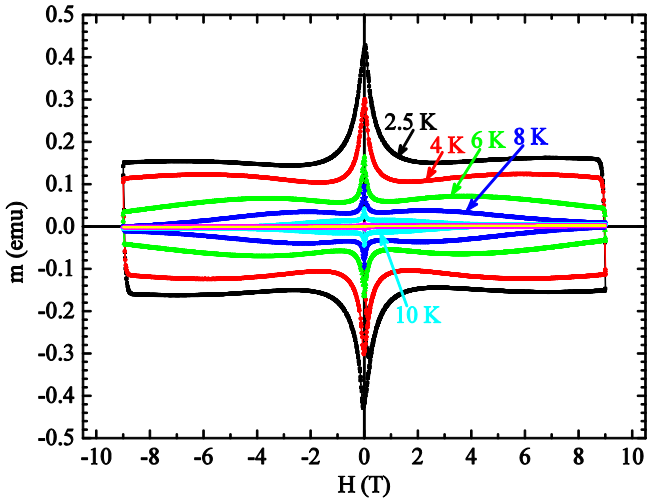

Figure 2. Superconducting hysteresis loops at different temperatures. The presence of the peak effect is visible.

reach +9 T, then back to −9 T, and finally to +9 T again in order to acquire the complete hysteresis loop.

3. Results and discussion

In order to determine the superconducting critical temperature T_c of our sample, an $M(T)$ measurement was performed in ZFC–FC conditions with an applied field of 0.01 T. The dc susceptibility curve $\chi_{dc}(T)$ was obtained from the $M(T)$ measurement, and the correction due to the demagnetization effects was also applied [62, 63] (the estimated demagnetizing factor is equal to 0.76). The result is shown in figure 1, where it can be noted that the sample exhibits a perfect diamagnetism with $\chi_{dc}(T = 2.5\,\text{K}) \approx -1$. The T_c was determined as the value of the temperature corresponding to the onset of the ZFC $\chi_{dc}(T)$ transition. As indicated in the inset of figure 1, where an enlargement of the curve in the region of the superconducting transition is shown, this value is approximately 14.5 K and it is consistent with the values reported in the literature [19, 52, 64–66]. It is worth underlining the presence of a non-zero signal above T_c in the ZFC magnetization, as well as a magnetic irreversibility between the ZFC and FC curves (see inset of figure 1). These characteristics may be ascribed to the existence of some magnetic impurities present in the sample, analogously to what was already reported in previous work on the FeSeTe system [49–52].

With the aim of investigating the superconducting and pinning properties of the sample, the $M(H)$ measurements were performed at different temperatures in the range between 2.5 K and 13 K. In figure 2 the measured curves are reported, and the presence of a 'peak effect' in the magnetization is clearly visible, and detectable up to the measurement temperature of 10 K. The evolution of this second peak, corresponding to the peak effect, has been analyzed by plotting the magnetic field values corresponding to it (H_{sp}) as a function

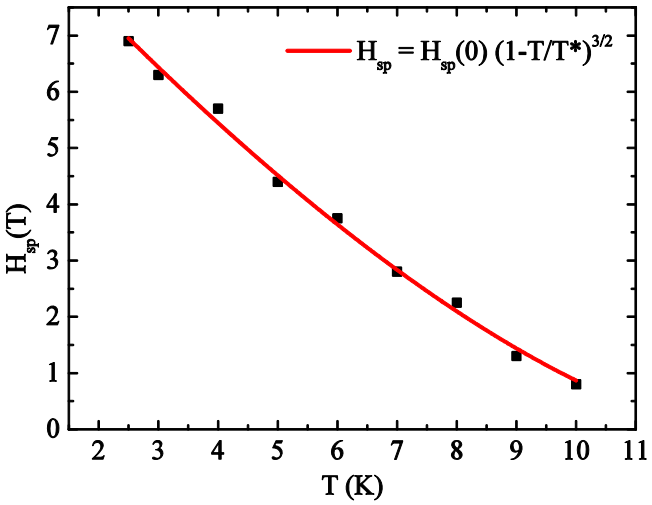

Figure 3. Temperature dependence of the magnetic field values corresponding to the second peak in the magnetization (H_{sp}). The red solid line is the fit of the data with equation $H_{sp} = H_{sp}(0)$ $(1 - T/T^*)^{3/2}$. Fit results are reported in the text.

of the temperature. This is shown in figure 3, where the decrease of H_{sp} with temperature can be observed. Its behavior appears similar to what has been reported for high T_c superconductors [67, 68], and it is possible to fit this $H_{sp}(T)$ curve with the expression $H_{sp} = H_{sp}(0)\,(1 - T/T^*)^{3/2}$, also used for IBSs [13, 37, 69, 70]. Here $H_{sp}(0)$ is the value of the magnetic field corresponding to the second peak in magnetization at $T = 0$ K, and T^* is the temperature where the peak is no longer detectable. From the fit, the values $H_{sp}(0) = 9.7 \pm 0.2$ T and $T^* = 12.5 \pm 0.3$ K are obtained. It is worth saying that, in spite of the value found for T^*, it was not possible to observe the presence of the peak effect in the curve measured at $T = 12$ K, likely due to the concurrence of the small superconducting signal close to T_c and a spurious magnetic signal coming from some magnetic impurities still present in our sample.

In order to study the peak effect phenomenon we focused our attention on the field and temperature dependencies of the

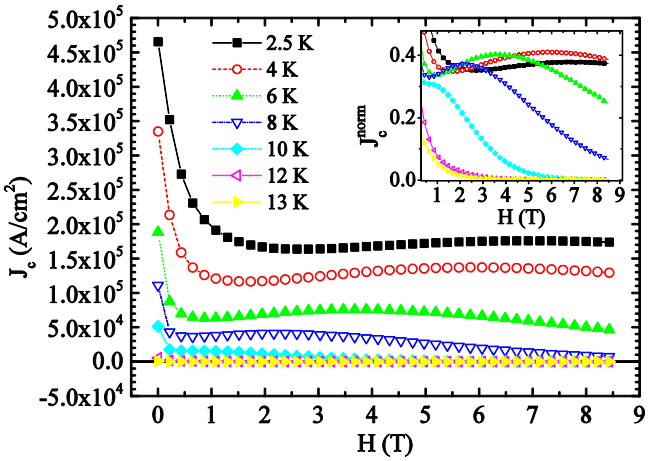

Figure 4. Critical current density J_c as a function of magnetic field at different temperatures extracted from the $M(H)$ curves of figure 2. Inset: enlargement of the normalized curves showing the shift of the second peak position towards lower magnetic fields by increasing the temperature.

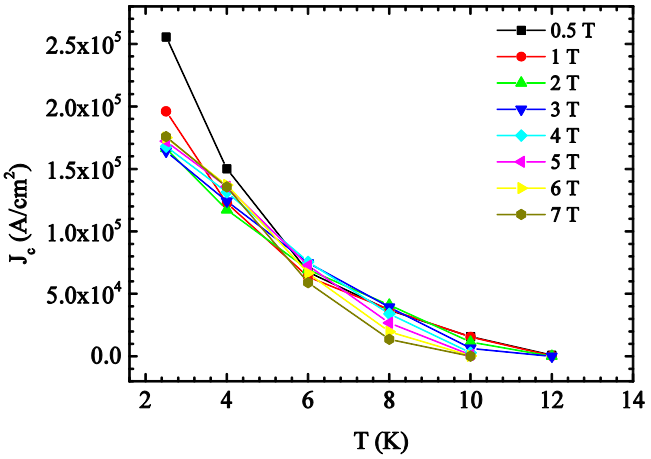

Figure 5. Temperature dependence of the critical current density J_c obtained by performing iso-field cuts of the $J_c(H)$ curves in figure 4. The solid lines are a guide for the eyes.

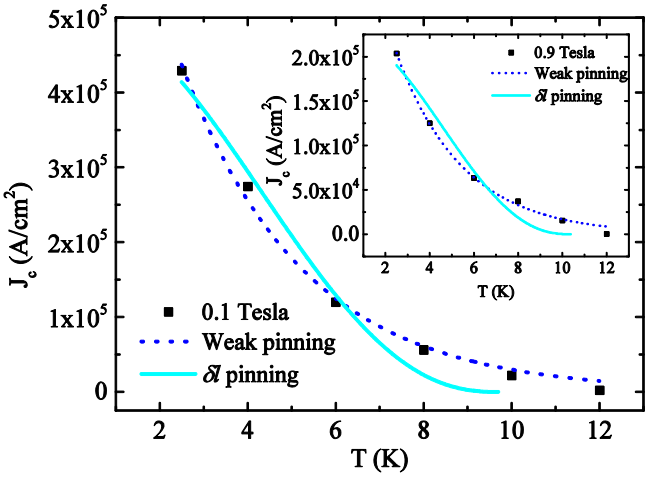

Figure 6. Temperature dependence of J_c at $H = 0.1$ T fitted with weak pinning (blue dotted line) and δl pinning (cyan solid line). Fit details are reported in the text. Inset: $J_c(T)$ at $H = 0.9$ T fitted with weak pinning (blue dotted line) and δl pinning (cyan solid line).

critical current density $J_c(H, T)$. From the $M(H)$ curves of figure 2, the critical current densities $J_c(H)$ have been calculated at different temperatures by using the Bean critical state model [71, 72]

$$J_c = \frac{20\Delta M}{\left[a\left(1 - \frac{a}{3b}\right)\right]} \quad (1)$$

where $\Delta M = M_{dn} - M_{up}$ is the difference between the magnetization measured for decreasing (M_{dn}) and increasing (M_{up}) applied field respectively, and a and b are the lengths (in cm) characterizing the cross section of the sample perpendicular to the applied field ($H||c$). The ΔM is measured in emu cm^{-3} and the calculated J_c is in A cm^{-2}. The obtained $J_c(H)$ curves are reported in figure 4 for different temperatures, and in the inset of figure 4 the shift of the peak effect in $J_c(H)$ to lower field with increasing temperature has been magnified. Our data do not allow us to appropriately use the Dew-Hughes analysis [39], due to the uncertainties in the evaluation of the irreversibility field H_{irr} in the region of interest. For this reason, by taking the value of J_c for certain fixed fields from the $J_c(H)$ curves at different temperatures, the $J_c(T)$ dependencies have been extracted in the entire field range from below to above the measured peak effect as reported in figure 5. To obtain information about the pinning regime acting in our sample, the $J_c(T)$ curves have been analyzed within several pinning models reported in the literature [1, 73–79]. At low magnetic field (H ranging from 0.1 T to 0.9 T), the best fit was obtained by using the equation describing the critical current in the presence of weak pinning centers, in particular considering lattice defects associated to point-like disorder or to in-plane dislocations inside the sample [1, 44, 45],

$$J_c^{weak}(T) = J_c^{weak}(0)\, e^{-T/T_0} \quad (2)$$

where $J_c^{weak}(0)$ is the value of J_c at T = 0 K, and T_0 is the characteristic pinning energy of weak (typically point-like) pinning defects. At this stage we could not determine the influence of the magnetic impurities on the pinning of the materials. However, the comparison of the properties of the sample analyzed in this work with those of an analogous $FeSe_{0.5}Te_{0.5}$ sample showing a larger magnetic background but lower J_c values [80] could suggest that there is not a productive correlation between the detected spurious magnetic signal and the pinning properties of the analyzed materials. In contrast to what was reported for the same material [27, 29, 33], as well as in the case of a different stoichiometry [37], a fit with the theoretical expression predicted in the presence of δl pinning was not satisfactory in our case in the low field region (see figure 6). For $H > 0.9$ T neither the weak pinning nor the δl pinning describe our data. In particular, the fit within the weak pinning scenario rapidly worsens as the magnetic field increases, thus indicating that the weak pinning centers' contribution to J_c starts to become negligible above 0.9 T.

A different situation is present in the high field region. In fact, in the range between 3 T and 8.5 T, the best fit of the

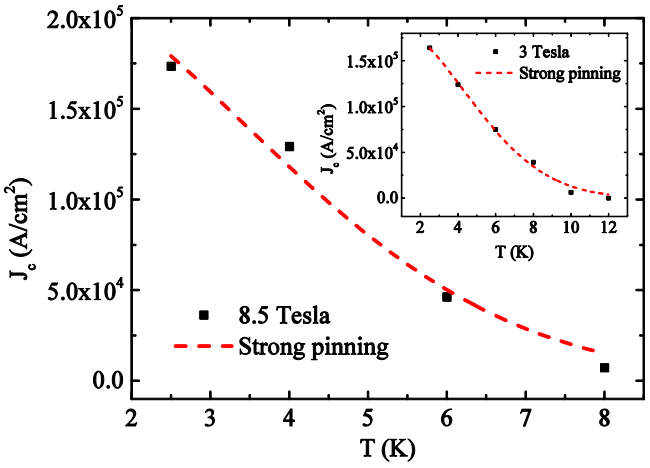

Figure 7. Temperature dependence of J_c at $H = 8.5$ T fitted with strong pinning (red dashed line). Fit details are reported in the text. Inset: $J_c(T)$ at $H = 3$ T fitted with strong pinning (red dashed line).

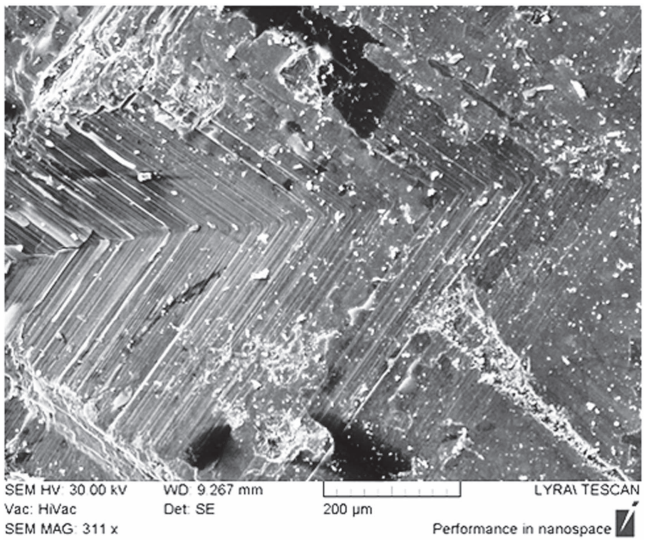

Figure 8. SEM image of the surface of the analyzed sample showing the presence of twin boundaries.

$J_c(T)$ curves is realized by considering the theoretical expression in the presence of strong pinning centers due to correlated disorder such as twin boundaries, columnar pins or defects [44, 46–48],

$$J_c^{str}(T) = J_c^{str}(0)e^{-3(T/T^*)^2} \quad (3)$$

where $J_c^{str}(0)$ characterizes the contribution to the J_c at $T = 0$ K and T^* is the vortex pinning energy of the strong pinning centers. The fit of the curves at $H = 8.5$ T and at $H = 3$ T with the strong pinning model is reported in figure 7 and in the inset of figure 7 respectively. For fields lower than 3 T, the strong pinning model starts to fail to describe satisfactorily the behavior of our data, its fits getting worse as the magnetic field decreases. It is important to underline that the morphological analysis performed on our sample (and on samples from the same batch) effectively confirms the presence of correlated disorder in terms of twin boundaries [31, 32, 46, 81] (see figure 8), which can act as strong pinning centers at high field in particular, where the point-like defects are not effective anymore.

The different pinning mechanisms that separately describe the critical current behavior for $H < 0.9$ T and for $H > 3$ T naturally suggest that in the intermediate region between these two fields the $J_c(T)$ can be described by a combination of the weak and the strong pinning contributions, expressed through the equation [44, 46]

$$J_c(T) = J_c^{weak}(0)e^{-T/T_0} + J_c^{str}(0)e^{-3(T/T^*)^2} \quad (4)$$

where $J_c^{weak}(0)$, $J_c^{str}(0)$, T_0 and T^* are the same parameters as in equations (2) and (3). The fitting procedure was applied to our data with equation (4) in the field range $1\text{ T} \leqslant H < 3\text{ T}$, by fixing the T_0 and T^* values obtained by the two separate previous fits and setting the critical current densities at $T = 0$ K as the only free parameter. An example of the obtained fits is reported in figure 9, just for the intermediate value of $H = 2$ T, but analogous results have been obtained for the other fields in this intermediate field range, suggesting that it represents a transition region between the weak pinning at the lowest fields and the strong pinning at the highest fields.

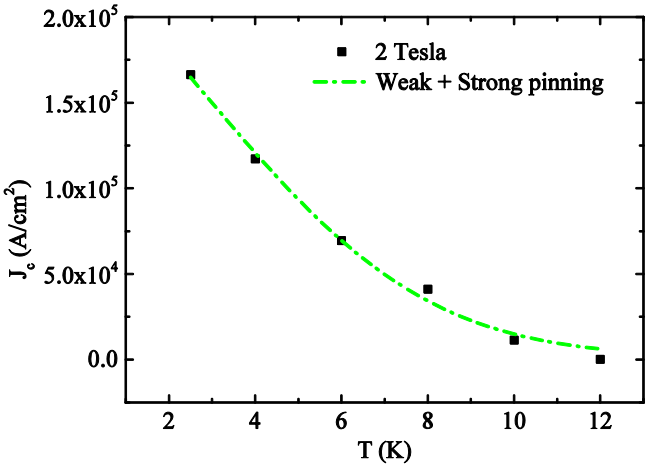

Figure 9. Temperature dependence of J_c at $H = 2$ T fitted with the combination of weak and strong pinning (dashed-dotted green line). Fit details are reported in the text.

We have to note that a similar picture of different coexisting pinning centers is observed using the Dew-Hughes $F_p(H/H_{irr})$ scaling approach applied to the pinning forces behavior in the FeSeTe [31].

From the fittings by equations (2), (3) and (4) it was possible to obtain the values of the parameters $J_c^{weak}(0)$, $J_c^{str}(0)$ and $J_c^{weak}(0) + J_c^{str}(0)$, respectively, i.e. the zero-temperature critical current densities $J_c(0)$ corresponding to the pinning mechanisms that we found to govern the magnetic response of our material in the range of fields and temperatures analyzed. The plot of these $J_c(0)$ values as functions of the magnetic field is reported in figure 10, where the sample can be seen to undergo a pinning crossover from the weak to the strong regime, which induces the peak effect visible in the enhancement of the critical current density at higher fields. On the basis of the experimental findings, we can therefore suppose that the detected magnetic behavior showing a peak effect in the critical current can be described by the following

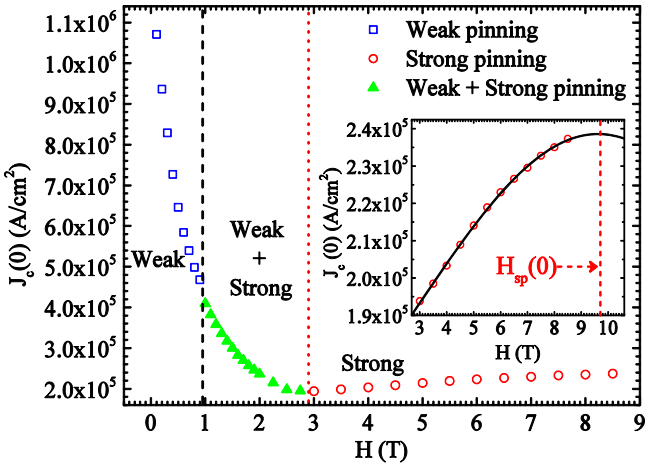

Figure 10. Field dependence of $J_c(0)$. The blue curve (empty squares) was obtained from the fit of the $J_c(T)$ data with weak pinning equation (2) for $H < 1$ T; the red curve (empty circles) was obtained from the fit of the $J_c(T)$ data with strong pinning equation (3) for $H \geqslant 3$ T; the green curve (full triangles) was obtained from the fit of the $J_c(T)$ data with the combination of weak and strong pinning equation (4) for $1\ \text{T} \leqslant H < 3$ T. Inset: a magnification of the $H \geqslant 3$ T region. The black solid line is the interpolation of the data with a Gaussian function. The red dashed line individuates the value of $H_{sp}(0)$ obtained by the fit showed in figure 3.

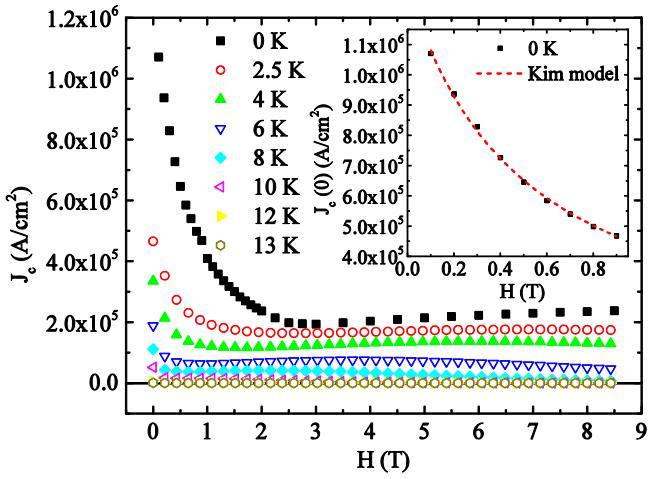

Figure 11. Critical current density J_c as a function of magnetic field at different temperatures, including $T = 0$ K. Inset: $J_c(0, H)$ fitted with the Kim model (red dashed line).

scenario: at low fields, vortices penetrate the material and get pinned by the point-like pinning centers which in principle are randomly distributed in the whole volume of the sample; as the field increases, the efficiency of these weak pinning centers reduces until it becomes too low to keep the vortex lattice pinned; the vortices start to escape from their pinning centers, thus reducing the critical current density, until they get trapped by the stronger pinning centers due to the correlated disorder of the twin boundaries; this second pinning mechanism causes the total pinning efficiency to increase again with increasing field, thus allowing the critical current to increase until it reaches a maximum value (at the field corresponding to the second peak in the magnetization loop) after which it naturally decreases as the field approaches H_{c2}. The correlation between peak effect and twin boundaries was already hypothesized for cuprates [81–83] and other IBSs [42, 84]. In this work, in addition to showing that this correlation exists for the FeSeTe superconductor, the role of the twin boundaries in the dynamical mechanism that produces the peak effect has been detected and described, by means of different pinning models corresponding to different field ranges. It is important to underline that at $H = 8.5$ T the $J_c(0)$ curve is still increasing (see figure 10). So, in order to create a guide for the eyes that allows one to identify the field $H^*(0)$ corresponding to the expected maximum in the $J_c(0)$ versus H curve, the region around its peak has been interpolated with a Gaussian function, which also interpolates the other $J_c(H)$ curves well for $T \neq 0$ around the peak. In the inset of figure 10 this interpolation is visible together with the original $J_c(0)$ data and with a vertical dashed line corresponding to the $H_{sp}(0)$ which in fact appears to be very close to $H^*(0)$. Moreover, if we also compare the qualitative behavior of $J_c(0)$ as a function of the magnetic field with the $J_c(H)$ at different temperatures, as shown in figure 11, we can observe that both the values and the trend of the curve at $T = 0$ K match well with the other curves at finite temperatures. Furthermore, the $J_c(0, H)$ curve at low magnetic fields (H ranging from 0.1 T to 0.9 T), has been well fitted with the dependence expressed in the Kim model [85–87] (see inset of figure 11), which is also plausible for describing the field behavior of a superconductor in the presence of an homogenous distribution of point-like defects. From the fit, the zero field and temperature critical current density $J_c(0, 0)$ has been extracted, its value being $J_c(0, 0) \approx 1.29 \times 10^6\ \text{A cm}^{-2}$.

All the features discussed up to here are summarized in an $H(T)$ phase diagram by plotting the characteristic fields H_{onset}, H_{sp}, H_{irr} and H_{c2} as shown in figure 12, where H_{onset} (blue solid squares) is the onset of the peak effect, H_{sp} (red solid circles) is the second peak position, H_{irr} (green solid triangles) is the irreversibility field determined from the $J_c(H)$ curves with the criterion of $J_c = 100\ \text{A cm}^{-2}$, and H_{c2} (magenta solid diamonds) is the upper critical field obtained by performing ZFC measurements at different magnetic fields. The corresponding behaviors are fitted with the expression $H(T) = H(0)\ (1 - T/T^*)^n$ where T^* is the temperature where the phenomena are no longer detectable. In particular, for the H_{c2} line, $T^* \equiv T_c$. The most relevant parameters obtained from the fitting procedure are $H_{onset}(0) = 3.8$ T and $n = 1.9$, $H_{sp}(0) = 9.7$ T and $n = 1.5$, $H_{irr}(0) = 39$ T and $n = 1.2$, and $H_{c2}(0) = 46.5$ T and $n = 1.4$ and they are in agreement with those reported for other IBSs [70, 88–90]. Below the $H_{onset}(T)$ line the material is characterized by weak/point-like pinning centers together with the beginning of the activation of the strong pinning centers. Between the $H_{onset}(T)$ and $H_{irr}(T)$ lines, a wide region of strong pinning characterizes the material, including the second peak line that usually identifies the crossover from elastic to plastic deformation [13–15]. In order to prove this crossover in our sample, the pinning energy has been extracted by measuring the magnetization as a function of

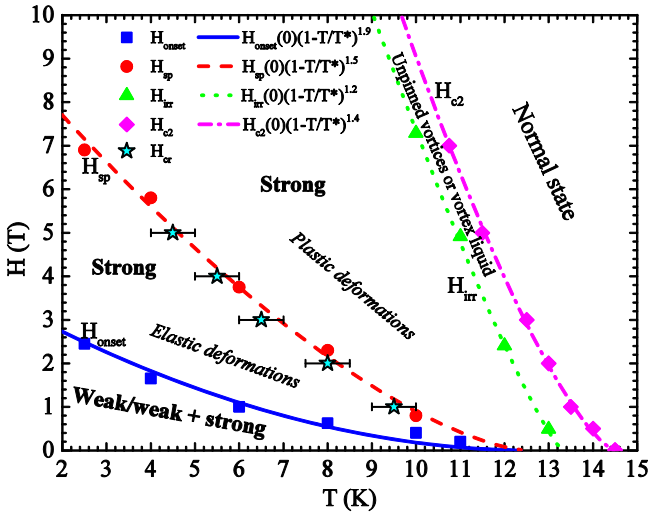

Figure 12. The $H(T)$ vortex phase diagram of $FeSe_{0.5}Te_{0.5}$ single twinned crystal. The characteristic field H_{onset} (blue solid squares) is the onset of the peak effect, H_{sp} (red solid circles) is the second peak position, H_{irr} (green solid triangles) is the irreversibility field, H_{c2} (magenta solid diamonds) is the upper critical field and the cyan stars represent the maxima in the $U(T)$ curves for different magnetic fields, $H_{cr}(T)$. The corresponding behaviors are fitted with the expression $H(T) = H(0)\ (1 - T/T^*)^n$. Fit details are reported in the text.

time $M(t)$ and using the relation $U = -T\ \mathrm{dln}(t)/\mathrm{dln}(|M|)$ [91, 92] to obtain the pinning energy as a function of temperature at different magnetic fields (not reported). The presence of a maximum in the $U(T)$ curves suggests a crossover, at given field and temperature $H_{cr}(T)$, from an elastic deformation of the lattice to a plastic one [92–95]. The $H_{cr}(T)$ values (indicated as cyan solid stars) have been plotted in the phase diagram of figure 12, and they lie satisfactorily on the second peak line, thus confirming that the maximum of the peak effect corresponds to a transition from the elastic to plastic deformation regime in the sample vortex lattice, followed by a decrease which is plausibly due to creep processes. Finally, it is important to observe that the irreversibility line is situated very close to the normal state line of H_{c2}, determining a very narrow liquid vortex state region, which is a distinct characteristic of a superconductor with dominant strong vortex pinning [42, 96].

4. Conclusions

By using dc magnetization measurements as function of temperature and dc magnetic field, we have analyzed the magnetic behavior of a $FeSe_{0.5}Te_{0.5}$ sample with critical temperature of 14.5 K fabricated by means of the Bridgman technique, where the presence of twin boundaries has been found. The existence of a correlation between this kind of defect and the appearance of a peak effect in the $M(H)$ curve has already been reported in the literature for various superconducting materials. The peak effect that we also observe in our $M(H)$ curves shows the same behavior as high T_c superconductors, with the field where the second peak appears decreasing for increasing temperature. Although the analysis of our results resembles the behavior of δl type pinning, the fit procedures suggest that a different pinning mechanism is responsible for the detected behaviors. Moreover, due to the relatively high temperatures with respect to T_c, where the peak effect is observed, the influence of quantum creep with respect to the classical creep has been neglected. On the other hand, the analysis of the $J_c(T)$ extracted from our measurements shows that the sample undergoes a pinning crossover with increasing H from a weak pinning regime, which is ascribed to the point defects homogenously distributed in the whole sample, to a strong pinning regime due to the presence of twin boundaries. This crossover appears to be responsible for the onset of the peak effect found in the $M(H)$ and in the extracted $J_c(H)$ curves, and the possible dynamic mechanism involving the contribution of the different pinning regimes depending on the applied field has been described. The scenario that has been used to interpret the experimental magnetic behavior allowed the analysis of the critical current density at low fields in terms of the Kim model, and so we obtained an estimation for J_c at zero field and temperature, and the field behavior of $J_c(T = 0\,\mathrm{K})$. The detected features have been used to draw the vortex phase diagram $H(T)$ with all the characteristic fields found in our analysis. The corresponding behaviors have been fitted with the equation $H(T) = H(0)\ (1 - T/T^*)^n$, allowing us to obtain the values of the related parameters which are in good agreement with those found in literature for the IBS systems. The second peak line has been analyzed by comparing its behavior with the temperature dependence of the pinning energy $U(T)$ at different magnetic fields. In this way we also confirm that the H_{sp} line can be interpreted as a transition from the elastic to plastic deformation regime in the vortex lattice, which determines the end of the growing process of the $J_c(H)$ corresponding to the maximum value of the critical current in the framework of the peak effect phenomenon.

Acknowledgments

This work has been carried out within the framework of the inter-academic Italian–Bulgarian research project (Department of Physics ‘E R Caianiello’ CNR-SPIN unit, University of Salerno and the Institute of Solid State Physics ‘Georgi Nadjakov’, Bulgarian Academy of Sciences). Two of the authors K Buchkov and E Nazarova acknowledge the financial support of project DFNP-158/13.05.2016 from the program for career development of young scientists. The authors would like to thank Prof. M Gospodinov from ISSP-BAS for valuable discussions and support for the sample preparation.

ORCID iDs

A Galluzzi https://orcid.org/0000-0002-1372-357X
M Polichetti https://orcid.org/0000-0002-4534-3301

References

[1] Blatter G, Geshkenbein V B, Larkin A I and Vinokur V M 1994 Vortices in high-temperature superconductors *Rev. Mod. Phys.* **66** 1125–388

[2] Brandt E H 2009 Vortices in superconductors: ideal lattice, pinning, and geometry effects *Supercond. Sci. Technol.* **22** 34019

[3] Kwok W-K, Welp U, Glatz A, Koshelev A E, Kihlstrom K J and Crabtree G W 2016 Vortices in high-performance high-temperature superconductors *Reports Prog. Phys.* **79** 116501

[4] Cohen L F, Laverty J R, Perkins G K, Caplin A D and Assmus W 1993 Fishtails, scales and magnetic fields *Cryogenics* **33** 352–6

[5] Jirsa M, Půst L, Dlouhý D and Koblischka M R 1997 Fishtail shape in the magnetic hysteresis loop for superconductors: interplay between different pinning mechanisms *Phys. Rev.* B **55** 3276–84

[6] Abulafia Y *et al* 1996 Plastic vortex creep in $YBa_2Cu_3O_{7-x}$ crystals *Phys. Rev. Lett.* **77** 1596–9

[7] Nishizaki T, Naito T and Kobayashi N 1998 Anomalous magnetization and field-driven disordering transition of a vortex lattice in untwinned $YBa_2Cu_3O_y$ *Phys. Rev.* B **58** 11169–72

[8] Li D P, Lin P-J, Rosenstein B, Shapiro B Y and Shapiro I 2006 Influence of quenched disorder on the square-to-rhombohedral structural transformation of the vortex lattice of type-II superconductors *Phys. Rev.* B **74** 174518

[9] Safar H, Gammel P L, Bishop D J, Mitzi D B and Kapitulnik A 1992 SQUID picovoltometry of single crystal $Bi_2Sr_2CaCu_2O_{8+\delta}$: observation of the crossover from high-temperature Arrhenius to low-temperature vortex-glass behavior *Phys. Rev. Lett.* **68** 2672–5

[10] Lortz R, Musolino N, Wang Y, Junod A and Toyota N 2007 Origin of the magnetization peak effect in the Nb_3Sn superconductor *Phys. Rev.* B **75** 94503

[11] Pissas M, Lee S, Yamamoto A and Tajima S 2002 Peak effect in single crystal MgB_2 superconductor for $H||c$ -axis *Phys. Rev. Lett.* **89** 97002

[12] Yang G, Shang P, Sutton S D, Jones I P, Abell J S and Gough C E 1993 Competing pinning mechanisms in $Bi_2Sr_2CaCu_2O_y$ single crystals by magnetic and defect structural studies *Phys. Rev.* B **48** 4054–60

[13] Yang H, Luo H, Wang Z and Wen H-H 2008 Fishtail effect and the vortex phase diagram of single crystal $Ba_{0.6}K_{0.4}Fe_2As_2$ *Appl. Phys. Lett.* **93** 142506

[14] Prozorov R *et al* 2008 Vortex phase diagram of $Ba(Fe_{0.93}Co_{0.07})_2As_2$ single crystals *Phys. Rev.* B **78** 224506

[15] Salem-Sugui S, Ghivelder L, Alvarenga A D, Cohen L F, Yates K A, Morrison K, Pimentel J L, Luo H, Wang Z and Wen H H 2010 Flux dynamics associated with the second magnetization peak in the iron pnictide $Ba_{1-x}K_xFe_2As_2$ *Phys. Rev.* B **82** 54513

[16] Pramanik A K, Harnagea L, Nacke C, Wolter A U B, Wurmehl S, Kataev V and Büchner B 2011 Fishtail effect and vortex dynamics in LiFeAs single crystals *Phys. Rev.* B **83** 94502

[17] Zhou W, Xing X, Wu W, Zhao H and Shi Z 2016 Second magnetization peak effect, vortex dynamics, and flux pinning in 112-type superconductor $Ca_{0.8}La_{0.2}Fe_{1-x}Co_xAs_2$ *Sci. Rep.* **6** 22278

[18] Taen T, Tsuchiya Y, Nakajima Y and Tamegai T 2009 Superconductivity at $T_c \sim 14$ K in single-crystalline $FeTe_{0.61}Se_{0.39}$ *Phys. Rev.* B **80** 92502

[19] Yeh K-W *et al* 2008 Tellurium substitution effect on superconductivity of the alpha-phase Iron Selenide *EPL* **84** 37002

[20] Hsu F-C *et al* 2008 Superconductivity in the PbO-type structure alpha-FeSe *Proc. Natl Acad. Sci. USA* **105** 14262–4

[21] Mizuguchi Y and Takano Y 2010 Review of Fe chalcogenides as the simplest Fe-based superconductor *J. Phys. Soc. Japan* **79** 102001

[22] Lei H, Wang K, Hu R, Ryu H, Abeykoon M, Bozin E S and Petrovic C 2012 Iron chalcogenide superconductors at high magnetic fields *Sci. Technol. Adv. Mater.* **13** 54305

[23] Si W, Han S J, Shi X, Ehrlich S N, Jaroszynski J, Goyal A and Li Q 2013 High current superconductivity in $FeSe_{0.5}Te_{0.5}$-coated conductors at 30 tesla *Nat. Commun.* **4** 1347

[24] Leo A *et al* 2015 Vortex pinning properties in Fe-chalcogenides *Supercond. Sci. Technol.* **28** 125001

[25] Yu Y, Wang C, Li Q, Wang H and Zhang C 2014 Vortex-glass phase transition and superconductivity in $Fe_{1.01}Te_{0.62}Se_{0.38}$ single crystal *J. Phys. Soc. Japan* **83** 114701

[26] Shahbazi M, Wang X L, Ghorbani S R, Dou S X and Lin C T 2015 Thermally activated flux flow in $Fe_{1.06}Te_{0.6}Se_{0.4}$ single crystal *Phys. C Supercond. its Appl.* **519** 60–4

[27] Klein T, Grasland H, Cercellier H, Toulemonde P and Marcenat C 2014 Vortex creep down to 0.3 K in superconducting Fe(Te, Se) single crystals *Phys. Rev.* B **89** 14514

[28] Liu T J *et al* 2009 Charge carrier localization induced by excess Fe in the Fe_{1+y}(Te, Se) superconductor system *Phys. Rev.* B **80** 174509

[29] Wu Z F, Wang Z H, Tao J, Qiu L, Yang S G and Wen H H 2016 Flux pinning and relaxation in $FeSe_{0.5}$ $Te_{0.5}$ single crystals *Supercond. Sci. Technol.* **29** 35006

[30] Miu D, Noji T, Adachi T, Koike Y and Miu L 2012 On the nature of the second magnetization peak in $FeSe_{1-x}Te_x$ single crystals *Supercond. Sci. Technol.* **25** 115009

[31] Hossaini S J, Ghorbani S R, Arabi H, Wang X L and Lin C T 2016 Temperature and field dependence of the flux pinning mechanisms in $Fe_{1.06}Te_{0.6}Se_{0.4}$ single crystal *Solid State Commun.* **246** 29–32

[32] Yadav C S and Paulose P L 2011 The flux pinning force and vortex phase diagram of single crystal *Solid State Commun.* **151** 216–8

[33] Das P, Thakur A D, Yadav A K, Tomy C V, Lees M R, Balakrishnan G, Ramakrishnan S and Grover A K 2011 Magnetization hysteresis and time decay measurements in $FeSe_{0.50}Te_{0.50}$: evidence for fluctuation in mean free path induced pinning *Phys. Rev.* B **84** 214526

[34] Shahbazi M, Wang X L, Dou S X, Fang H and Lin C T 2013 The flux pinning mechanism, and electrical and magnetic anisotropy in $Fe_{1.04}Te_{0.6}Se_{0.4}$ superconducting single crystal *J. Appl. Phys.* **113** 17E115

[35] Tamegai T, Sun Y, Yamada T and Pyon S 2016 Critical current density and vortex dynamics in Fe(Te, Se) annealed in various atmosphere *IEEE Trans. Appl. Supercond.* **26** 1–5

[36] Sun Y, Taen T, Tsuchiya Y, Pyon S, Shi Z and Tamegai T 2013 Magnetic relaxation and collective vortex creep in $FeTe_{0.6}Se_{0.4}$ single crystal *EPL* **103** 57013

[37] Bonura M, Giannini E, Viennois R and Senatore C 2012 Temperature and time scaling of the peak-effect vortex configuration in $FeTe_{0.7}Se_{0.3}$ *Phys. Rev.* B **85** 134532

[38] Liu Y, Kremer R K and Lin C T 2010 Superconductivity and vortex pinning in $Fe_{1.04}Te_{0.60}Se_{0.40}$ single crystal *EPL* **92** 57004

[39] Dew-Hughes D 1974 Flux pinning mechanisms in type II superconductors *Philos. Mag.* **30** 293–305

[40] Larkin A I, Marchetti M C and Vinokur V M 1995 Peak effect in twinned superconductors *Phys. Rev. Lett.* **75** 2992–5

[41] Kwok W K, Fleshler S, Welp U, Vinokur V M, Downey J, Crabtree G W and Miller M M 1992 Vortex lattice melting

in untwinned and twinned single crystals of $YBa_2Cu_3O_{7-\delta}$ *Phys. Rev. Lett.* **69** 3370–3

[42] Marziali Bermúdez M, Pasquini G, Bud'ko S L and Canfield P C 2013 Correlated vortex pinning in slightly orthorhombic twinned $Ba(Fe_{1-x}Co_x)_2As_2$ single crystals: possible shift of the vortex-glass/liquid transition *Phys. Rev.* B **87** 54515

[43] Song C-L, Wang Y-L, Jiang Y-P, Wang L, He K, Chen X, Hoffman J E, Ma X-C and Xue Q-K 2012 Suppression of superconductivity by twin boundaries in FeSe *Phys. Rev. Lett.* **109** 137004

[44] Polat A, Sinclair J W, Zuev Y L, Thompson J R, Christen D K, Cook S W, Kumar D, Chen Y and Selvamanickam V 2011 Thickness dependence of magnetic relaxation and E-J characteristics in superconducting (Gd-Y)-Ba-Cu-O films with strong vortex pinning *Phys. Rev.* B **84** 24519

[45] Christen D K and Thompson R 1993 Current problems at high T_c *Nature* **364** 98–9

[46] Plain J, Puig T, Sandiumenge F, Obradors X and Rabier J 2002 Microstructural influence on critical currents and irreversibility line in melt-textured $YBa_2Cu_3O_{7-x}$ reannealed at high oxygen pressure *Phys. Rev.* B **65** 104526

[47] Nelson D R and Vinokur V M 1993 Boson localization and correlated pinning of superconducting vortex arrays *Phys. Rev.* B **48** 13060–97

[48] Hwa T, Le Doussal P, Nelson D R and Vinokur V M 1993 Flux pinning and forced vortex entanglement by splayed columnar defects *Phys. Rev. Lett.* **71** 3545–8

[49] Tsurkan V, Deisenhofer J, Günther A, Kant C, Klemm M, von Nidda H-A, Schrettle F and Loidl A 2011 Physical properties of $FeSe_{0.5}Te_{0.5}$ single crystals grown under different conditions *Eur. Phys. J.* B **79** 289–99

[50] Wittlin A, Aleshkevych P, Przybylińska H, Gawryluk D J, Dłużewski P, Berkowski M, Puźniak R, Gutowska M U and Wiśniewski A 2012 Microstructural magnetic phases in superconducting $FeTe_{0.65}$ $Se_{0.35}$ *Supercond. Sci. Technol.* **25** 65019

[51] Sivakov A G *et al* 2017 Microstructural and transport properties of superconducting $FeTe_{0.65}$ $Se_{0.35}$ crystals *Supercond. Sci. Technol.* **30** 15018

[52] Fiamozzi Zignani C, De Marzi G, Grimaldi G, Leo A, Guarino A, Vannozzi A, della Corte A and Pace S 2017 Fabrication and physical properties of polycrystalline iron-chalcogenides superconductors *IEEE Trans. Appl. Supercond.* **27** 1–5

[53] McQueen T M *et al* 2009 Extreme sensitivity of superconductivity to stoichiometry in $Fe_{1+\delta}Se$ *Phys. Rev.* B **79** 14522

[54] Onar K and Yakinci M E 2015 Solid state synthesis and characterization of bulk β-FeSe superconductors *J. Alloys Compd.* **620** 210–6

[55] Fiamozzi Zignani C *et al* 2016 Fabrication and characterization of sintered iron-chalcogenide superconductors *IEEE Trans. Appl. Supercond.* **26** 1–5

[56] Gömöry F 1997 Characterization of high-temperature superconductors by AC susceptibility measurements *Supercond. Sci. Technol.* **10** 523–42

[57] Polichetti M, Adesso M G and Pace S 2004 Response of glass and liquid phases in the vortex lattice to an external AC magnetic field at different frequencies *Physica* A **339** 119–24

[58] Hein R, Francavilla T and Liebenberg D 1991 *Magnetic Susceptibility of Superconductors and Other Spin Systems* ed R A Hein *et al* (Boston, MA: Springer US)

[59] Senatore C, Polichetti M, Clayton N, Flükiger R and Pace S 2004 Non-linear magnetic response of MgB_2 bulk superconductors *J. Phys.* C **401** 182–6

[60] Zola D, Polichetti M, Senatore C and Pace S 2004 Magnetic relaxation of type-II superconductors in a mixed state of entrapped and shielded flux *Phys. Rev.* B **70** 224504

[61] Galluzzi A, Polichetti M, Buchkov K, Nazarova E, Mancusi D and Pace S 2015 Evaluation of the intragrain critical current density in a multidomain FeSe crystal by means of dc magnetic measurements *Supercond. Sci. Technol.* **28** 115005

[62] Stoner E C 1945 XCVII. The demagnetizing factors for ellipsoids *Philos. Mag. J. Sci.* **36** 803–21

[63] Prando G, Giraud R, Aswartham S, Vakaliuk O, Abdel-Hafiez M, Hess C, Wurmehl S, Wolter A U B and Büchner B 2013 Evidence for a vortex–glass transition in superconducting $Ba(Fe_{0.9}Co_{0.1})_2As_2$ *J. Phys. Condens. Matter* **25** 505701

[64] Mizuguchi Y, Tomioka F, Tsuda S, Yamaguchi T and Takano Y 2009 Substitution effects on FeSe superconductor *J. Phys. Soc. Japan* **78** 74712

[65] Sales B C, Sefat A S, McGuire M A, Jin R Y, Mandrus D and Mozharivskyj Y 2009 Bulk superconductivity at 14 K in single crystals of $Fe_{1+y}Te_xSe_{1-x}$ *Phys. Rev.* B **79** 94521

[66] Putti M *et al* 2009 New Fe-based superconductors: properties relevant for applications *Supercond. Sci. Technol.* **23** 34003

[67] Zhukov A A, Küpfer H, Perkins G, Cohen L F, Caplin A D, Klestov S A, Claus H, Voronkova V I, Wolf T and Wühl H 1995 Influence of oxygen stoichiometry on the irreversible magnetization and flux creep in $RBa_2Cu_3O_{7-\delta}$ (R = Y, Tm) single crystals *Phys. Rev.* B **51** 12704–14

[68] Klein L, Yacoby E R, Yeshurun Y, Erb A, Muller-Vogt G, Breit V and Wuhl H 1994 Peak effect and scaling of irreversible properties in untwinned Y-Ba-Cn-O crystals *Phys. Rev.* B **49** 4403

[69] Pramanik A K, Aswartham S, Wolter A U B, Wurmehl S, Kataev V and Büchner B 2013 Flux dynamics and avalanches in the 122 pnictide superconductor $Ba_{0.65}Na_{0.35}Fe_2As_2$ *J. Phys. Condens. Matter* **25** 495701

[70] Shen B, Cheng P, Wang Z, Fang L, Ren C, Shan L and Wen H H 2010 Flux dynamics and vortex phase diagram in $Ba(Fe_{1-x}Co_x)_2As_2$ single crystals revealed by magnetization and its relaxation *Phys. Rev.* B **81** 14503

[71] Bean C P 1962 Magnetization of hard superconductors *Phys. Rev. Lett.* **8** 250–3

[72] Bean C P 1964 Magnetization of high-field superconductors *Rev. Mod. Phys.* **36** 31–9

[73] Griessen R, Wen H-H, van Dalen A J J, Dam B, Rector J and Schnack H G 1994 Evidence for mean free path fluctuation induced pinning in $YBa_2Cu_3O_7$ and $YBa_2Cu_4O_8$ films *Phys. Rev. Lett.* **72** 1910–3

[74] Savvides N 1990 Flux creep and transport critical current density in high-Tc superconductors *J. Phys.* C **165** 371–6

[75] Murakami M, Fujimoto H, Gotoh S, Yamaguchi K, Koshizuka N and Tanaka S 1991 Flux pinning due to nonsuperconducting particles in melt processed YBaCuO superconductors *J. Phys.* C **185–189** 321–6

[76] Yeshurun Y and Malozemoff A P 1988 Giant flux creep and irreversibility in an Y-Ba-Cu-O crystal: an alternative to the superconducting-glass model *Phys. Rev. Lett.* **60** 2202–5

[77] Jackson D J C and Das M P 1996 Melting of the flux line lattice *Supercond. Sci. Technol.* **9** 713–27

[78] Yom S S, Hahn T S, Kim Y H, Chu H and Choi S S 1989 Exponential temperature dependence of the critical transport current in Y-Ba-Cu-O thin films *Appl. Phys. Lett.* **54** 2370

[79] Hsiang T Y and Finnemore D K 1980 Superconducting critical currents for thick, clean superconductor—normal-metal—superconductor junctions *Phys. Rev.* B **22** 154–63

[80] Galluzzi A, Buchkov K, Tomov V, Nazarova E, Leo A, Grimaldi G, Pace S and Polichetti M 2017 private communication

[81] Suematsu H, Okamura H, Nagaya S and Yamauchi H 1999 Role of the twin boundary for the occurrence of peak effect in Y-Ba-Cu-O superconducting bulks melt grown under varied oxygen pressure *Supercond. Sci. Technol.* **12** 274–81
[82] Palau A, Durrell J H, MacManus-Driscoll J L, Harrington S, Puig T, Sandiumenge F, Obradors X and Blamire M G 2006 Crossover between channeling and pinning at twin boundaries in $YBa_2Cu_3O_7$ thin films *Phys. Rev. Lett.* **97** 257002
[83] Suematsu H, Okamura H, Lee S, Nagaya S and Yamauchi H 2000 A possible cause of the peak effect in Y–Ba–Cu–O melt-grown bulks: modulation in oxygen distribution *J. Phys.* C **338** 96–102
[84] Shen B, Yang H, Zeng B, Ren C, Xu X and Wen H-H 2011 Multiple Magnetization Peaks and New Type of Vortex Phase Transitions in $Ba_{0.6}K_{0.4}Fe_2As_2$ (arXiv:1111.6105)
[85] Kim Y B, Hempstead C F and Strnad A R 1962 Critical persistent currents in hard superconductors *Phys. Rev. Lett.* **9** 306–9
[86] Kim Y B, Hempstead C F and Strnad A R 1963 Magnetization and critical supercurrents *Phys. Rev.* **129** 528–35
[87] Poole C P 2007 *Superconductivity* (Amsterdam: Elsevier)
[88] Shahbazi M, Wang X L, Choi K Y and Dou S X 2013 Flux pinning mechanism in $BaFe_{1.9}Ni_{0.1}As_2$ single crystals: evidence for fluctuation in mean free path induced pinning *Cit. Appl. Phys. Lett* **103**
[89] Jiao Y, Cheng W, Deng Q, Yang H and Wen H-H 2017 Collective vortex pinning and crossover between second order to first order transition in optimally doped $Ba_{1-x}K_xBiO_3$ single crystals (arXiv:1701.01346)
[90] Leo A *et al* 2017 Quenching current by flux-flow instability in iron-chalcogenides thin films *IEEE Trans. Appl. Supercond.* **27** 1–5
[91] Yeshurun Y, Malozemoff A and Shaulov A 1996 Magnetic relaxation in high-temperature superconductors *Rev. Mod. Phys.* **68** 911–49
[92] Galluzzi A, Polichetti M, Buchkov K, Nazarova E, Mancusi D and Pace S 2017 Critical current and flux dynamics in Ag-doped FeSe superconductor *Supercond. Sci. Technol.* **30** 025013
[93] Miu L and Miu D 2010 On the sensitivity of the Maley technique for the analysis of vortex-creep activation energy in disordered superconductors *Supercond. Sci. Technol.* **23** 025033
[94] Miu L, Miu D, Petrisor T, El Tahan A, Jakob G and Adrian H 2008 Origin of the plateau in the temperature dependence of the normalized magnetization relaxation rate in disordered high-temperature superconductors *Phys. Rev.* B **78** 212508
[95] El Tahan A, Jakob G, Miu D, Ivan I, Badica P and Miu L 2011 Vortex creep crossover in YBCO/PrBCO superlattices during standard magnetization relaxation measurements *Supercond. Sci. Technol.* **24** 045014
[96] Yamamoto A *et al* 2009 Small anisotropy, weak thermal fluctuations, and high field superconductivity in Co-doped iron pnictide $Ba(Fe_{1-x}Co_x)_2As_2$ *Appl. Phys. Lett.* **94** 62511